Role of Hydration Sphere on ^{7}Li NMR Images of Stressed Porous Disk

Subhendra N. Sarkar

NMR Laboratory, Depts. of Radiology and Pathology, University of Arkansas for Medical Sciences, Little Rock, AR 72205

Nuclear magnetic resonance (NMR) imaging of fluids in porous materials has offered nondestructive mapping of sub-millimeter-size or larger structures (Sarkar et al., 1991; Sarkar et al., 1992; Tutunjian et al., 1991; Edelstein et al., 1988). Interfacial phenomena are difficult to address by NMR imaging due to lack of sensitivity.

For fluids in porous media, the longitudinal magnetization in the main field direction is perturbed substantially by long-range interactions via coupled rotation or restricted diffusion of molecules (Fung and McGaughy, 1981). Measurement of longitudinal magnetization decay rate (time constant T_1) and corresponding T_1-weighted NMR images, therefore, can be used to fingerprint fluid location and possibly the interaction with the pore surfaces.

On the other hand, transverse magnetization is affected mainly by short-range interactions arising from:

1.   The magnetic field anisotropy of instrumental origin and magnetic susceptibility differences inherent in a hetero-geneous medium (Fung and McGaughy, 1981)

2.   The motion of other nuclear spins physically or chemically associated with the spins of interest.

Since the first factor cannot be easily estimated or eliminated, information from T_2-weighted images of millimeter-size resolution is of limited use today.

Large difference between T_1 and T_2 values for brine nuclei in porous systems (Tutunjian et al., 1991; Sarkar et al., 1992) suggests relaxations far from motional narrowing range typical in pure liquids, and both dipolar and quadrupolar relaxations are operative. For the spin 3/2 ^{7}Li nuclei, however, a weak quadrupolar interaction in bulk solution is not well understood (Lindman and Forsen, 1978; Webb, 1978).

Oil recovery by brine injection in oil well cores is quite common, and a knowledge about porosity and phase com-patibility in core plugs as well as brine wettability of residual oil-wet pores can enhance efficiency of current oil recovery methods. NMR studies of alkali ions after such a flood can directly locate the residual brine phase (Tutunjian et al., 1991; Sarkar et al., 1992). However, NMR signals from brine nuclei in dilute core floods is about two orders of magnitude weaker than ^{1}H signals from solvent due to their low gyromagnetic ratios and low concentration (Komoroski and Sarkar, 1991; Tutunjian et al., 1991).

The low T_1 values for brine nuclei in porous media (< 1 s) enable fast co-addition of NMR scans, and moderately low T_2s (> 1 ms) permit acquisition of useful NMR images by low echo time (TE) imaging sequences (Tutunjian et al., 1991; Sarkar et al., 1992).

One thrust behind this work is the hypothesis that since alkali ions interact directly with pore surfaces, suitably designed NMR imaging of these ions may offer information about interfacial interaction. It is observed that ^{7}Li NMR images of LiCl so-lutions in silica contain intensity contrast in mechanically stressed pores. This was explained from the stress-enhanced diffusivity of water dipoles which makes the coupling between surface layers and the bulk solvent more efficient. Expected applications include stress detection in geological and reservoir rock samples.

Experimental Studies

A 4-mm-thick sintered glass disk, 35% porosity and 170-220 μm controlled pore size (from Kontes, Vineland, NJ), was used for flooding with 2-, 4- and 8-M aqueous LiCl brine. One edge of the disk was rubbed with sand paper for about 10 minutes and two holes (1.6 mm and 2 mm in diameters) were drilled at its center fast and without using any cooling fluid. After correcting for the weight loss due to drilling and me-chanical roughing, the new pore volume available for external fluid intake was found to decrease by about 4%. This was attributed to an increase in the fraction of isolated pores near the drilled region due to the heat generated from dry drilling.

Next, the disk was placed in a beaker inside a vacuum des-sicator at 100 mtorr of pressure followed by LiCl brine injection (vacuum imbibition). After each imaging experiment, the disk was soaked in de-ionized water for a day and was boiled for 1 h to bring down the residual NMR peak intensity of ^{7}Li to less than 1% of initial value. This was followed by drying at 70°C and then imbibing with another brine concentration.

The ^{7}Li NMR imaging was done in a General Electric Omega CSI-4.7T system at ^{7}Li Larmor frequency of 77.7 MHz using

Acustar shielded medium-high gradients (up to a maximum of 20 g/cm). A 60 mm × 80 mm birdcage volume coil was used for both excitation and detection. A 3-D whole volume imaging sequence (Sarkar and Komoroski, 1992) with an echo time of 1 ms was employed for obtaining four slices to cover the entire thickness of the sample resulting in $0.5 \times 0.5 \times 1$ mm^3 image resolution. Using 4, 2 and 1 scans per data point and 3 s for scan repetition time (TR), ^{7}Li multislice NMR images with good S/N were acquired in 100, 50 and 25 min for 2-, 4- and 8-M LiCl flooded disk, respectively.

The T_1 and T_2 of ^{7}Li NMR signals from the whole disk were obtained using inversion recovery and Hahn spin-echo sequences. T_1s near the drilled holes were estimated from exponentially decaying one-dimensional intensity profiles by varying scan repetition times and regional T_2s from the same region were estimated by varying echo times in the imaging sequence.

Results and Discussion

Table 1 shows a collection of ^{7}Li relaxation times. Note that T_1 from the whole sample decreases, and T_2 increases with increasing concentration of LiCl flood. The reason for this T_2 increase seems to be due to a greater fraction of ^{7}Li nuclei available after concentrated floods in the bulk of the pores having some motional freedom compared to dilute LiCl where a greater fraction of ^{7}Li nuclei is perhaps associated with the surfaces. From the single exponential T_2 data, however, the role of surfaces cannot be confirmed. The main discussion below, therefore, will be based on interpreting T_1 dependence in the NMR data.

The lowering of T_1 as seen here is not expected from diffusion-controlled translational motion of ^{7}Li nuclei. The diffusion coefficient of insufficiently hydrated Li$^+$ ions in concentrated LiCl solutions in bulk is slightly more than that of highly hydrated Li$^+$ ions in dilute LiCl solutions and should contribute toward a slight increase in T_1. The rotational correlation time of hydrated Li$^+$ complex also is inversely proportional to the dipolar part of T_1. A reasonable estimate for rotational correlation time of hydrated Li$^+$ complex is about 1×10^{-12} s (Lindman and Forsen, 1978). A twofold reduction in the size of the hydrated Li$^+$ means a twofold reduction in the rotational correlation time and a corresponding increase in T_1. Therefore, the decrease in T_1 in this sample, as the solution becomes more concentrated, has to be attributed to new types of dipolar or enhanced quadrupolar interaction.

Regional T_1s and T_2s estimated around the holes are shorter than the bulk values resulting in T_1 ratios of 2.3, 1.9 and 1.1

Table 1. NMR Relaxation Times for ^{7}Li in LiCl-Flooded Porous Glass Disk

Conc. of ag LiCl Flood (M)	T_1 (ms) of Whole Sample	Local T_1 (ms)*	T_2 (ms) of Whole Sample	Local T_2 (ms)**
2	2,650	1,160	55	20
4	1,930	1,020	120	60
8	910	820	175	85

*Estimated from exponential growth in total NMR intensity profiles in a 5-mm-thick transverse slice containing drilled holes as scan repetition times are varied between 0.1 and 30 s.
**Estimated from exponential decay in total NMR intensity profiles of the same slice by varying echo times between 0.5 to 500 ms.
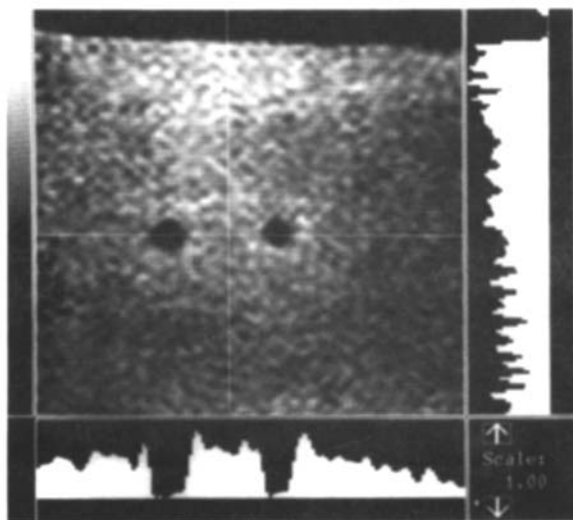
for 2-, 4- and 8-M floods, respectively. Since the NMR signal is proportional to $\exp [1 - e^{-TR/T_1}]e^{-TE/T_2}$, all the images are primarily T_1-weighted and virtually T_2-insensitive at $TE = 1$ ms. Hence, it is unnecessary to discuss T_2s in detail.

Due to a symmetric hydration shell, ^{7}Li responds weakly to electric field gradients (Webb, 1978; Lindman and Forsen, 1978) and forms hydrogen bonds in a dipolar environment up to several layers at the pore surfaces. Note that ^{7}Li T_1s in porous disk are not too low compared to T_1s in bulk solutions (2-15 s for 8-2-M LiCl in bulk, Lindman and Forsen, 1978). This is expected since the bulk volume of the pores far exceeds total surface area and the surface layers cannot lower the ^{7}Li T_1 drastically on the basis of usual dipolar relaxation mechanism.

Possible quadrupolar T_1 relaxation pathways for ^{7}Li in porous glass could be due to:

(1) Quadrupolar interactions of incompletely hydrated Li$^+$ with other Li$^+$ and Cl$^-$ counterions in the bulk volume of the pores.

(2) Quadrupolar interaction of surface bound Li$^+$(H$_2$O)$_n$ species with unbalanced charges around the active surface silanol sites.

Normal diffusivity of water allows at most 0.1 μm distance around a Li$^+$ ion to exchange water dipoles during an NMR scan. This effect should be maximum for dilute LiCl solutions which can provide free solvent to help grow a dense region of silanol functionalities (SiOH $-$) in these pore surfaces and form multiple hydrogen bonds in all directions. Each Li$^+$ ion in such a cage of water dipoles undergoes efficient quadrupolar relaxation. A large number of Li$^+$, Cl$^-$ pairs present in 4- and 8-M solutions compete among themselves for hydrating water and cannot produce this effect at the pore surfaces. However, the dominance of quadrupolar interaction in concentrated solutions at the bulk of a pore seems to lower T_1 severely and more than compensates for the lack of a thick surface layer. Hence, both the dipolar and quadrupolar pathways at the pore surfaces cannot change the average values of T_1 measured mainly from the species in the bulk.

Representative central image slices from all three LiCl flood concentrations are shown in Figures 1 to 3. Note the difference in intensity as the LiCl concentration is changed from 2 M to 8 M. Higher intensity in several voxels around the drilled holes and at the top edge for 2-M LiCl-flooded disk occurs from a faster recovery of ^{7}Li longitudinal magnetization vector compared to the rest of the disk. The T_1 contrast for 4-M flood is moderate and for 8-M flood the image is almost uniform. In light of various pathways for T_1 relaxation, this is analyzed as follows:

(1) There is no reason why quadrupolar mechanism at the bulk of the stressed pores will be modified compared to the unstressed regions since stress reduces T_1 in 8-M solution only by 10%.

(2) Perhaps one should reconsider the dipolar mechanism and the surface effects since the stress-induced T_1 reduction is most significant in dilute brine flood (approximately 60% reduction).

It may be inferred from the decrease in externally accessible pore volume after drilling that mechanical stress has caused a reduction of pore-throat connectivities in the stressed regions leading to fluid unsaturated pores and available vapor phase therein. Kenyon et al. (1982) have simulated role of trapped

Figure 1. Central slice and intensity projections across cursor lines of a T_1-weighted, but T_2-independent (since TE = 1 ms) ^{7}Li NMR image set of the porous disk flooded by 2-M aq LiCl.

Drilled holes are visible as dark spots; image resolution is $0.5 \times 0.5 \times 1$ mm^3.

air in unsaturated pores on T_1 values in sandstones. Here, glass tubes of radii < 200 μm have been used to simulate unsaturated pores (with saturation factor $S < 1$). The resulting ratio $T_1(S)/T_1(S=1) \sim S^{1/3}$ for fast diffusing species and $T_1(S)/T_1(S=1) \sim S^{2/3}$ for slowly diffusing species may be applicable here. For a saturation factor of 0.4, for example, the fast moving Li$^+$ (with smaller hydration shell in 8-M solution) gives this T_1 ratio as 0.7, implying less signal contrast. For well hydrated, bulky and slow-moving Li$^+$ ions (in 2-M LiCl), this ratio equals 0.5, suggesting a twofold intensity difference in T_1-weighted images as observed here.
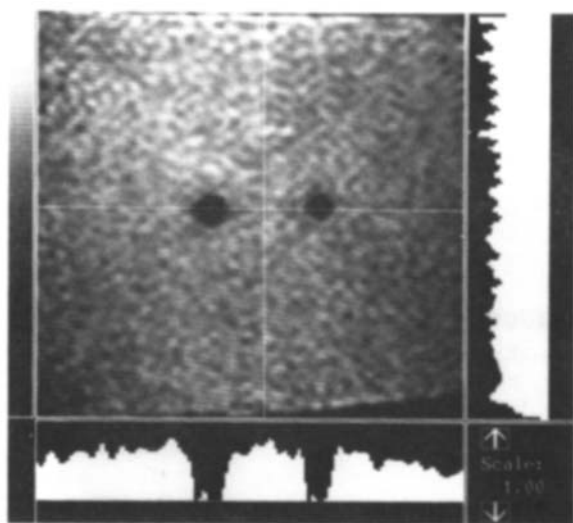

Figure 2. Same slice and same resolution as in Figure 1 from the ^{7}Li NMR image set of silica disk flooded by 4-M LiCl: TE = 1 ms.
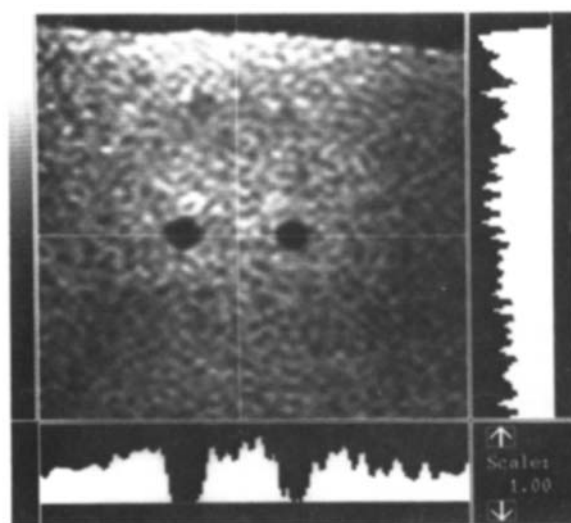

Figure 3. Central slice as in Figures 1 and 2 of the glass disk flooded by 8-M LiCl brine: TE = 1 ms.

Therefore, modeling of a thicker surface layer for dilute LiCl flood has to be supplemented by the presence of many partially saturated pores around the drilled region to explain the T_1 contrast satisfactorily.

A significant enhancement of self-diffusion lengths of water dipoles in partially filled pores (D'Orazio et al., 1989), not of Li$^+$ themselves, will cause transfer of water dipoles from the hydrated Li$^+$ to the vapor phase enabling each ^{7}Li nucleus to sample dipolar relaxation from many more water dipoles (for example, from 200-μm-dia. whole pore) contrasted with the 0.1-μm limit in the absence of a vapor phase. Note that the high frequency for releasing water dipoles from the hydrated shells of Li$^+$ in gas phase (200 MHz; Burgess, 1988) is the main driving force for the enhanced self-diffusion of water in brine unsaturated pores. Again, there is not enough free water to exchange with vapor phase, and enhanced self-diffusion of water is not possible due to high viscosity in the case of concentrated brine floods.

Conclusions

Direct NMR imaging of ^{7}Li nuclei from $\geq$ 2-M LiCl-saturated silica by short TE imaging sequence provides images with submillimeter resolutions in a few minutes. T_1s of ^{7}Li nuclei in porous media are an order of magnitude lower than T_1s in solution due to restricted motion in pores. Measured T_1 values for ^{7}Li in porous media are dominated by the values at the bulk of the pores, and the role of active surfaces cannot be determined easily by NMR.

Mechanical stress causes open porosity loss in model silica matrix, and about 10% to 60% reduction in ^{7}Li T_1 is observed in the stressed region depending on the concentration of aqueous LiCl solution used to saturate the matrix. This may be explained by modeling an enhanced dipolar interaction extending from the stressed pore surfaces to the bulk of those pores via fast exchange of solvent dipoles with the vapor phase. Therefore, a greater T_1 contrast in the brine images of dilute brine floods can perhaps be used to detect stress in geothermal

or petrophysical environments of paramagnetics-free porous media.

Notation

T_1 = characteristic longitudinal magnetization decay time in NMR
T_2 = characteristic transverse magnetization decay time in NMR
TE = time to form echo in spin-echo NMR pulse sequence
TR = repetition time for NMR scans used for signal averaging

Literature Cited

Burgess, J., "Ion-Solvent Interaction," *Ions in Solution*, Ellis Horwood Ltd., Chichester, UK, Chap. 4, 45 (1988).

D'Orazio, F., S. Bhattacharja, W. P. Halperin, and R. Gerhardt, "Enhanced Self-Diffusion of Water in Restricted Geometry," *Phys. Rev. Lett.*, **63**, 43 (1989).

Edelstein, W. A., H. J. Vinegar, P. N. Tutunjian, P. B. Roemer, and

O. M. Mueller, "NMR Imaging for Core Analysis," *Technical Conf., Soc. Petr. Eng.*, No. 18272, Houston (1988).

Fung, B. M., and T. W. McGaughy, "Magnetic Relaxation in Heterogeneous Systems," *J. Magn. Reson.*, **43**, 316 (1981).

Kenyon, W. E., P. I. Day, C. Straley, and J. F. Willemsen, "A Three-Part Study of NMR Longitudinal Relaxatior Properties of Water-Saturated Sandstones," *Soc. Petr. Eng. J. Form. Eval.*, **3**, 622 (1982).

Komoroski, R. A., and S. N. Sarkar, "NMR Imaging of Elastomers and Porous Media," *Proc. Mat. Res. Soc.*, **217**, 3 (1991).

Lindman, B., and S. Forsen, *NMR and the Periodic Table*, p. 129, R. K. Harris and B. E. Mann, eds., Academic Press, New York (1978).

Sarkar, S. N., W. E. Wooten, and R. A. Komoroski, "NMR Imaging of Water in Model Porous Materials," *Appl. Spectroscopy*, **45**, 619 (1991).

Sarkar, S. N., R. A. Komoroski, and J. J. Dechter, "Multinuclear NMR Imaging of Porous Materials and Rock Core Samples," *Conf. Anal. Chem. & Spectrosc.*, No. 798, New Orleans (1992).

Sarkar, S. N., and R. A. Komoroski, "NMR Imaging of Morphology, Defects, and Composition of Tire Composites and Model Elastomer Blends," *Macromolec.*, **25**, 1420 (1992).

Tutunjian, P. N., H. J. Vinegar, and J. A. Ferris, "Nuclear Magnetic Resonance Imaging of Sodium-23 in Cores," *Tech. Conf. Soc. Core Analysts*, No. 9111, San Antonio (1991).

Webb, G. A., *NMR and the Periodic Table*, p. 75, R. K. Harris and B. E. Mann, eds., Academic Press, New York (1978).